THE ASTRONOMICAL JOURNAL, 121:2572–2583, 2001 May
© 2001. The American Astronomical Society. All rights reserved. Printed in U.S.A.

RADIAL VELOCITY OF THE PHOENIX DWARF GALAXY: LINKING STARS AND H I GAS[1]

C. GALLART,[2,3] D. MARTÍNEZ-DELGADO,[4] M. A. GÓMEZ-FLECHOSO,[5] AND M. MATEO[6]

Received 2000 November 6; accepted 2001 February 8

ABSTRACT

We present the first radial velocity measurement of the stellar component of the Local Group dwarf galaxy Phoenix, using the FORS1 instrument at the VLT's Unit Telescope 1 (Antu). From the spectra of 31 red giant branch stars, we derive a heliocentric optical radial velocity for Phoenix of $V_\odot = -52 \pm 6$ km s^{-1}. On the basis of this velocity, and taking into account the results of a series of semianalytical and numerical simulations, we discuss the possible association of the H I clouds observed in the Phoenix vicinity. We conclude that the characteristics of the H I cloud with heliocentric velocity -23 km s^{-1} are consistent with this gas having been associated with Phoenix in the past and being lost by the galaxy after the last event of star formation in the galaxy, about 100 Myr ago. Two possible scenarios are discussed: the ejection of the gas by the energy released by the supernovae (SNe) produced in that last event of star formation and a ram pressure stripping scenario. We derive that the kinetic energy necessary to eject the gas is $E_{\rm SNe} \sim 2 \times 10^{51}$ ergs and that the number of SNe necessary to transfer this amount of kinetic energy to the gas cloud is $\sim$20. This is consistent with the number of SNe expected for the last event of star formation in Phoenix, according to the star formation history derived by Martínez-Delgado, Gallart, & Aparicio. The drawback of this scenario is the regular appearance of the H I cloud and its anisotropic distribution with respect to the stellar component. Another possibility is that the H I gas was stripped as a consequence of ram pressure by the intergalactic medium. In our simulations, the structure of the gas remains quite smooth as it is stripped from Phoenix, keeping a distribution similar to that of the observed H I cloud. Both in the SNe ejection case and in the ram pressure sweeping scenario, the distances and relative velocities imply that the H I cloud is not gravitationally bound to Phoenix, since this would require a Phoenix total mass about an order of magnitude larger than its total estimated mass. Finally, we discuss the possibility that Phoenix may be a bound Milky Way satellite. The minimum required mass of the Milky Way for Phoenix to be bound is $M_{\rm MW}$ ($<$450 kpc) $\geq 1.2 \times 10^{12}\ M_\odot$, which comfortably fits within most current estimates.

Key words: galaxies: dwarf — galaxies: evolution — galaxies: individual (Phoenix Dwarf) — ISM: H I — Local Group

1. INTRODUCTION

At the low end of the mass and luminosity distributions, dwarf galaxies are the most common type of galaxies in the universe. They are usually divided in two groups: dwarf irregular (dIrr) galaxies and dwarf spheroidal (dSph) galaxies. In the simplest scheme, the key differences between the two groups is that dIrr galaxies have large amounts of gas and substantial current star formation activity, while dSph galaxies lack gas and recent star formation. However, this picture has been shown to be too simplistic, and the distinction between the two classes is not always straightforward. There are dIrr galaxies such as LGS 3 (Aparicio, Gallart, & Bertelli 1997b; Young & Lo 1997) and Pegasus (Aparicio et al. 1997a; Lo, Sargent, & Young 1993), with substantial amounts of gas but apparently low star formation rate. Other galaxies, such as Fornax and Leo I, which are traditionally considered dSph galaxies have relatively recent (few hundred million year old) star formation (Stetson, Hesser, & Smecker-Hane 1998; Gallart et al. 1999a, 1999b). Finally, there are some interesting cases where gas, not centered in the optical component of the galaxy, is or may be associated with dSph systems: Sculptor (Carignan et al. 1998), Tucana (Oosterloo, Da Costa, & Staveley-Smith 1996), And III, And V, Leo I, and Sextans (Blitz & Robishaw 2000).

From the theoretical point of view, the relationship between dIrr and dSph galaxies and their possible evolutionary links have been profusely discussed in the literature (e.g., Einasto et al. 1974; Lin & Faber 1983; Dekel & Silk 1986; Silk, Wyse, & Shields 1987; Davies & Phillips 1989; Mac Low & Ferrara 1999; Ferrara & Tolstoy 2000). The fact that the same basic relations and overall structure are shared by dIrr and dSph galaxies (Binggeli 1994) seem to point to a common origin. On the other hand, the morphological segregation of dwarfs, with dSph galaxies in general close to large galaxies and preferentially isolated dIrr galaxies (van den Bergh 1994), may suggest some kind of environmentally driven evolution, either related to ram pressure sweeping (Lin & Faber 1983) or enhanced star formation that rapidly consumed the gas in high-density environments (Davies & Phillips 1989; Lacey & Silk 1991).

Phoenix has the characteristics of a system in which a transition from a dIrr to a dSph galaxy may be currently going on. It shows recent star formation in its central part (500 to 100 Myr ago), but no H I has been observed centered

[1] Based on observations collected in visitor mode with the VLT UT1, Antu, at the European Southern Observatory, Chile.

[2] Departamento de Astronomía, Universidad de Chile, Casilla 36-D, Las Condes, Santiago, Chile.

[3] Andes Prize Fellow, Department of Astronomy, Yale University, P.O. Box 208101, New Haven, CT 06520-8101.

[4] Instituto de Astrofísica de Canarias, Via Lactea, E-38200 La Laguna, Tenerife, Spain.

[5] Observatoire de Genève, CH-1290 Sauverny, Switzerland.

[6] Department of Astronomy, 821 Dennison Building, University of Michigan, Ann Arbor, MI 48109.

in the optical galaxy. Nevertheless, several clouds at different radial velocities have been detected close to it. Carignan, Demers, & Côté (1991) detected H I emission at $V_\odot = 56$ km s^{-1} which was clearly separated from a much larger scale component at ~ 120 km s^{-1} associated with the Magellanic Stream. Oosterloo et al. (1996) detected another smaller cloud at $V_\odot = -23$ km s^{-1}, situated 6′ southwest from the center of the galaxy. VLA observations by Young & Lo (1997) confirmed the existence of this last cloud close to the optical galaxy, forming a curved structure that wraps around its southwest border. Subsequently, St-Germain et al. (1999) reobserved a $2^\circ \times 2^\circ$ area around Phoenix with the Australia Telescope Compact Array, remapping all the previously observed components, plus one at 7 km s^{-1} that is likely of Galactic origin. After a thorough discussion of all available evidence, these authors conclude that, because of its compact shape and internal velocity gradient, the amount of H I mass ($\simeq 10^5\ M_\odot$) derived for the cloud if at the distance of the galaxy, and its location, almost overlapping the southwest outskirts of Phoenix, the -23 km s^{-1} component is the one most likely associated with Phoenix. It is interesting that the spatial variation of the young population with age in Phoenix is consistent with a possible self-propagation of the star formation over its disk from east to west (Martínez-Delgado, Gallart, & Aparicio 1999; see also Held, Saviane, & Momany 1999). Therefore, if the -23 km s^{-1} component were to prove to be associated with Phoenix, it would provide tantalizing evidence that a burst of star formation may blow out the gas from a dwarf galaxy. However, without a measurement of the radial velocity of the Phoenix stellar component, it is not possible to establish a reliable connection between the stars and the H I gas seen near Phoenix in projection.

We present here the first measurement of the radial velocity of the stellar component in Phoenix and discuss the possible association between the galaxy and the gas clouds in its neighborhood in the sky. This paper is organized as follows: In § 2, we present the spectroscopic observations performed with FORS1 at VLT-Antu. The derivation of the radial velocities of the Phoenix red giant branch (RGB) stars is described in § 3. Finally, the implications of the derived Phoenix radial velocity regarding the possible association with the galaxy of the different H I clouds detected toward it is discussed in § 4, based on the results of

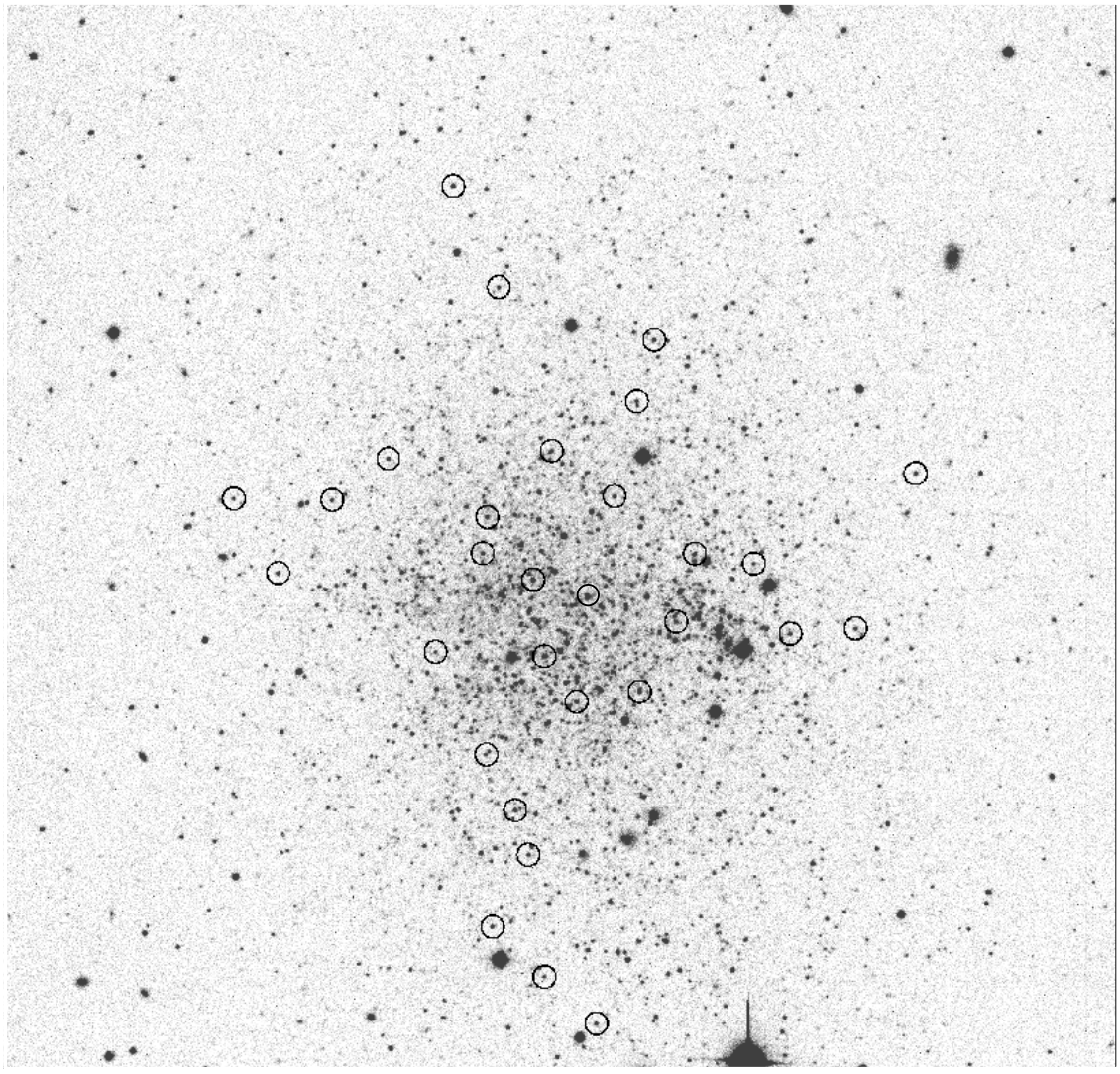


FIG. 1.—Identification chart for the stars measured in Phoenix. The image is a 120 s V exposure at the VLT. North is up, and east is to the left.

TABLE 1

OBSERVING LOG FOR THE PHOENIX AND VELOCITY STANDARD STARS

Object	α (J2000.0)	δ (J2000.0)	Archive File	Exp. Time (s)
HD 176047 No. 1.....	18 59 44.12	−34 28 14	FORS.1999-09-14T23:44:30.357.fits	10
HD 176047 No. 2.....	18 59 44.12	−34 28 14	FORS.1999-09-14T23:48:29.001.fits	20
HD $176047_{\text{sky No. 1}}$.....	18 59 45.73	−34 28 14	FORS.1999-09-14T23:51:50.492.fits	300
HD 176047 No. 3.....	18 59 44.12	−34 28 14	FORS.1999-09-15T00:00:21.868.fits	150
HD $176047_{\text{sky No. 2}}$.....	18 59 45.73	−34 28 14	FORS.1999-09-15T00:06:18.654.fits	600
HD 196983 No. 1.....	20 41 48.98	−33 53 16	FORS.1999-09-15T00:24:57.582.fits	240
HD $196983_{\text{sky No. 1}}$.....	20 41 47.44	−33 53 16	FORS.1999-09-15T00:34:39.793.fits	300
HD 196983 No. 2.....	20 41 48.98	−33 53 16	FORS.1999-09-15T01:21:13.492.fits	240
HD 196983 No. 3.....	20 41 48.98	−33 53 16	FORS.1999-09-15T01:28:43.540.fits	120
HD $196983_{\text{sky No. 2}}$.....	20 41 50.69	−33 52 57	FORS.1999-09-15T01:34:41.289.fits	600
HD 203638	21 24 07.99	−20 50 59	FORS.1999-09-15T03:39:29.409.fits	5
HD 203638_{sky}	21 24 09.27	−20 50 59	FORS.1999-09-15T03:42:16.512.fits	600
Phoenix set 1.....	01 51 04	−44 26 05	FORS.1999-09-15T06:03:47.856.fits	1500
			FORS.1999-09-15T06:30:32.498.fits	1500
			FORS.1999-09-15T06:57:17.324.fits	1500
Phoenix set 2.1.....	01 50 57	−44 26 40	FORS.1999-09-15T07:34:53.935.fits	1500
			FORS.1999-09-15T08:01:38.649.fits	900
Phoenix set 2.2.....	01 50 57	−44 26 40	FORS.1999-09-15T08:18:01.062.fits	1800
			FORS.1999-09-15T08:49:45.413.fits	1800
cpd432597 No. 1.....	06 32 13.20	−43 31 14	FORS.1999-09-15T09:45:44.645.fits	12
cpd432597 No. 2.....	06 32 13.20	−43 31 14	FORS.1999-09-15T09:48:03.264.fits	48

NOTE.—Units of right ascension are hours, minutes, and seconds, and units of declination are degrees, arcminutes, and arcseconds.

semianalytical and numerical simulations of supernova explosions and ram pressure stripping scenarios. Our conclusions are summarized in § 5.

2. OBSERVATIONS

Spectroscopy of a sample of candidate Phoenix stars and several velocity standard stars was obtained with the Focal Reducer/Low Dispersion Spectrograph (FORS1) at VLT-Antu on the night of 1999 September 14/15. The observing conditions were apparently photometric, but the seeing was mediocre, about 1″–1.″5 the whole night with some improvement only at the end of the night, down to 0.″7.

We knew from past experience that, even for red giant stars, the best spectral range to observe them for radial velocity measurements purposes is between about 450–530 nm (Vogt et al. 1995). In this region, even for relatively metal-poor stars, we obtain the highest density of spectral lines, adequate continuum stellar flux, and low sky emission. We extended the spectral coverage some more to the red to include some skylines, in particular [O I] λ5577, to set the zero point of the wavelength calibration. In FORS1, the grism that covers that spectral region is GRIS-600B. Its spectral resolution is $R = 815$, which, with a resolution of 50 Å mm^{-1} and a CCD pixel size of 24 μm, gave a dispersion of 1.2 Å pixel^{-1}.

We observed in multislit mode (MOS) to obtain spectroscopy of a sample of stars in the field of Phoenix (Fig. 1). The usable field of view of 6.′8 × 4′ basically covered the main body of the galaxy. In two MOS setups (see Tables 1 and 5 and Figs. 2 and 3), we were able to employ 14 and 16 slitlets

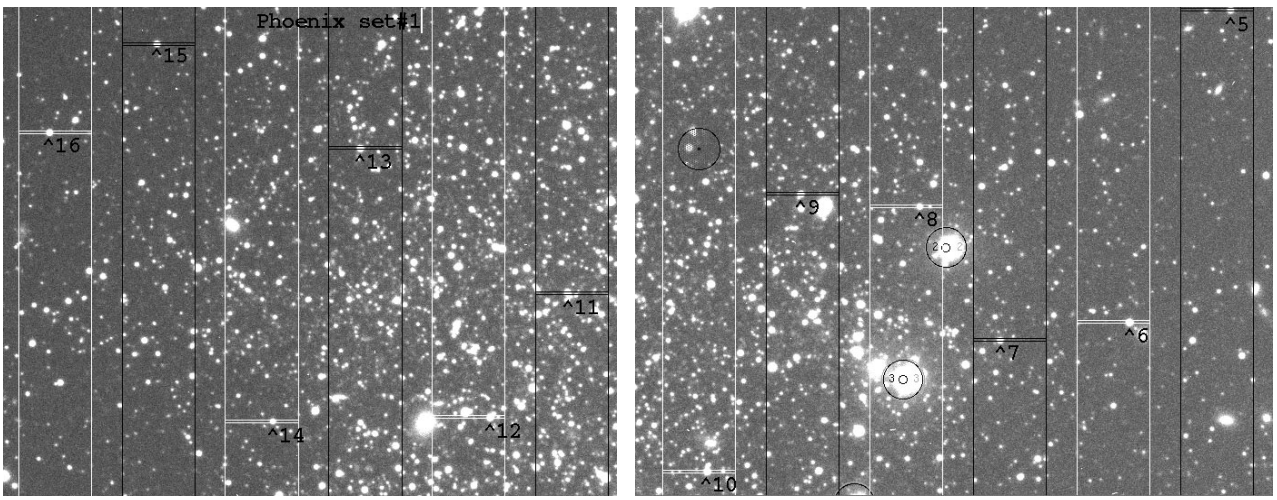


FIG. 2.—MOS setup configuration for Phoenix set 1 (Table 1). FORS1 reference stars are circled. North is up, and east is to the left.

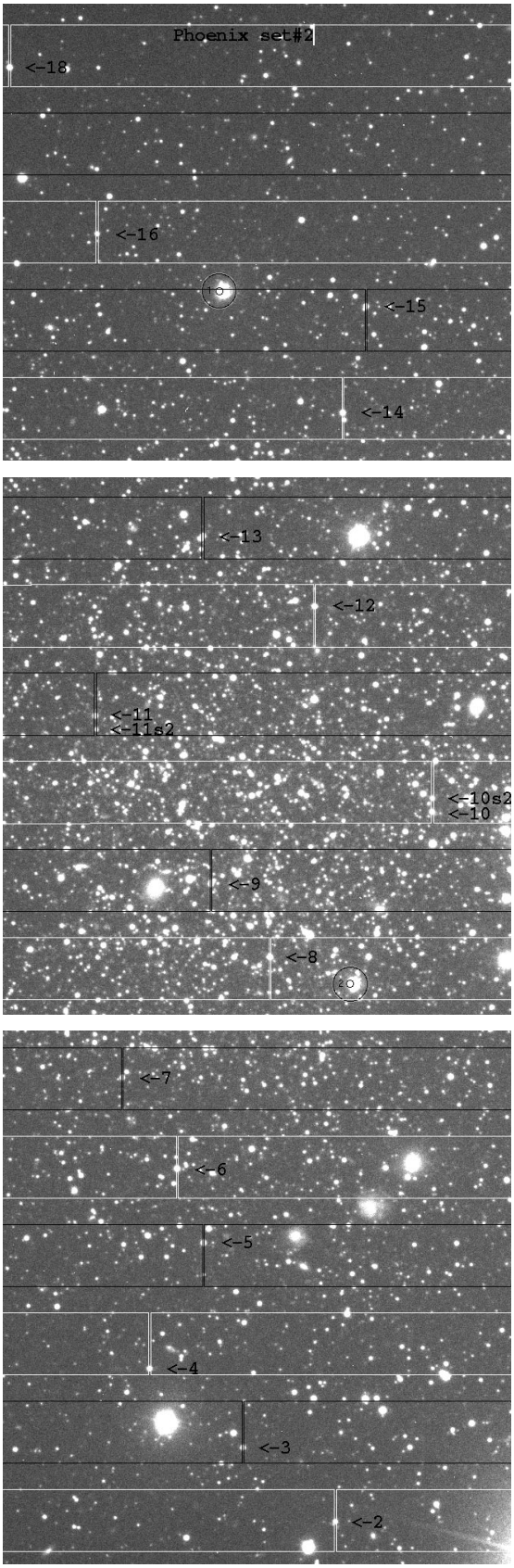


FIG. 3.—MOS setup configuration for Phoenix set 2 (Table 1). FORS1 reference stars are also marked. North is up, and east is to the left.

on stars that had a very high probability of membership as red giants in the galaxy, as selected from the Martínez-Delgado et al. (1999) photometry. A second star happened to be aligned with the selected target star in two of the slitlets of the second set. Figure 4 shows a Phoenix color-magnitude diagram (CMD) with the observed stars marked.

We prepared approximate MOS slitlet configurations using the FIMS VLT software and the Las Campanas image of Phoenix used in Martínez-Delgado et al. (1999). This image did not allow positioning the slitlets with enough precision to actually perform the observations, but it did allow to select optimal configurations of the 19 slitlet set to secure maximum occupancy by the brightest red giants. The night before our observations, A. Iovino (who was observing before us with FORS1) kindly took a 120 s *V* FORS1 image of Phoenix for us, with which we were able to refine the slitlet positioning in such a way that no further adjustments were necessary during the target acquisition at the telescope.

Four velocity standards of spectral type K0–K3 were observed a total of nine times through the night. Because the exposure times necessary to obtain good signal-to-noise ratio (S/N) spectra of the standard stars were short to provide a good measurement of the position of the 5577 Å O I line, we took, immediately after each standard-star measurement, a companion spectra of the sky, with exposure times of 300–600 s. These companion spectra proved indeed very useful to obtain reliable corrections of the zero point of our wavelength calibration. Table 2 identifies the standard stars observed and lists the velocity measurements. In addition, we took a 300 s exposure of the twilight sky to be used as an extra, high-S/N velocity template.

Arcs and screen flat fields were taken in the morning after our observations in each MOS setup. For practical considerations, the obtention of calibration arcs during the night is not supported with FORS1. This is because the whole operation of recording a wavelength calibration spectrum at night requires approximately 30 minutes. Because it

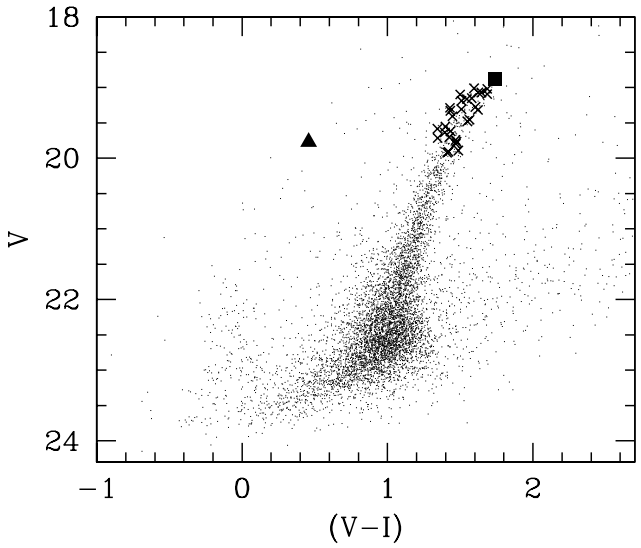


FIG. 4.—CMD of Phoenix, with the measured stars near the tip of the red giant branch identified (*crosses*). The C star and the bright supergiant (late-B to early-A spectral type) star (see the Appendix) are identified with a square and a triangle, respectively.

TABLE 2

RADIAL VELOCITY STANDARDS

Star	V_{obs}	R	σ_v	V_{helio}	$V_{helio} - V_{obs}$
HD 176047 No. 1.....	−40.8	91.42	4.9	−42.8	−2.0
HD 176047 No. 2.....	−46.1	112.64	4.0	−42.8	3.3
HD 176047 No. 3.....	−42.6	115.85	3.0	−42.8	0.2
HD 196983 No. 1.....	5.2	62.45	7.2	−9.3	−14.5
HD 196983 No. 2.....	−15.2	98.44	4.6	−9.3	5.9
HD 196983 No. 3.....	−10.1	79.65	5.6	−9.3	0.8
HD 203638	10.6	63.17	7.1	21.9	11.3

[a] The standard-star radial velocities were taken from the following references: HD 176047 and HD 196983, Maurice et al. 1984; HD 203638, Astronomical Almanac 1999.

involves a reconfiguration of the telescope and of the instrument, it does not offer any significant advantage, compared with next morning daytime calibrations, in terms of stability of the configuration with respect to the one used for the observation of the scientific target. Therefore, the use of arc lamp spectra is restricted to defining the dispersion relation while zero-point alignment is more accurately achieved using the night skylines as references.

3. VELOCITY MEASUREMENTS

3.1. *Basic Reduction Procedures*

Because this is our first paper reporting radial velocity measurements using FORS1 at the VLT, we will describe our reduction techniques in some detail. This section may be skipped by any readers uninterested in the precise reduction procedure. We mainly used routines from the EXPORT version V2.11 of Sun/IRAF, with occasional use of MIDAS routines.

1. The data were taken in single-amplifier mode and high gain (0.68 e^- ADU^{-1} and 5.03 e^- readout noise). We used IRAF to remove the bias level from the images, by using a set of bias frames taken in the same mode, plus the overscan region of each image.

2. Screen flat fields were obtained in each slitlet configuration using the two available sets (blue and red filtered) of halogen flat-field lamps. Four flat fields were averaged for each configuration using IRAF and subsequently normalized using NORM/MOS within the MIDAS package. This routine averages the rows separately for each slitlet, smooths with a median filter (of 10 pixels here), and divides each row of the slitlet by the filtered average. The division of each object frame by the corresponding flat field was performed using IRAF.

3. Three 1500 s exposures were obtained in one of the slitlets configurations while two sets (1500 + 900 s and 2 × 1800 s) were obtained in the second. No noticeable shifts were detected in either the spatial or the dispersion direction, and the spectra in each set were averaged to increase S/N and eliminate cosmic rays.

4. Individual two-dimensional spectra were cut from the FORS1 image. From these, one-dimensional spectra were extracted using the NOAO.TWODSPEC.APEXTRACT.APALL package in IRAF. At this point we also subtracted the sky background by fitting it across the dispersion at either side of the star spectrum. The subtracted sky spectrum was kept in one of the beams of the multispec format for possible use at a later phase to refine the wavelength calibration using skylines.

5. He + HgCd lamp calibration spectra in each slitlet configuration were obtained the morning after the Phoenix and standard stars' observations and were extracted, except for the background subtraction, with parameters identical to those for the object spectra. We used NOAO.ONEDSPEC.IDENTIFY to identify the lines in each calibration spectrum. Order 4 Chebyshev polynomials were typically fitted to the position of 11–14 spectral lines, and the derived transformations were applied to the program objects using the NOAO.ONEDSPEC.DISPCOR package.

6. The wavelength calibration zero point was checked and refined using the [O I] line at 5577.34 Å. This line is present with high S/N in all Phoenix long-exposure spectra, but it is too faint in the radial velocity standard-star spectra to provide a reliable measure of its position. For them, we used the longer exposure spectra obtained after shifting slightly the pointing of the telescope to remove the standard star from the slitlet (see Table 1). The center of the 5577 Å line was obtained by fitting a Gaussian profile using NOAO.ONEDSPEC.SPLOT. The fact that there is some correlation between the position of the telescope and the amount and sign of the shift (see Table 3) gives us confidence that we are indeed measuring an actual effect of telescope or instrument flexures on the spectra. The calculated $\delta\lambda = 5577.34 - \lambda_{obs}$ shifts, typically within ±0.4 Å (Table 3), were applied to both Phoenix and standard stars' images by modifying the CRVAL1 header parameter, which provides the starting wavelength of each spectra.

7. The spectra were continuum-subtracted using NOAO.ONEDSPEC.CONTINUUM. Finally, for the Phoenix spectra, we removed all pixels with $40 \leq$ values ≤ -40 by replacing them with 0.0 using IMAGES.IMUTIL.IMREPLACE to get rid of any sky residuals and remaining cosmic rays.

3.2. *The Master Radial Velocity Template*

We combined the standard star's observations plus the twilight solar spectra into a single high-S/N master template spectrum. To do this, we first transformed these spectra to a $\log \lambda$ scale using NOAO.ONEDSPEC.DISPCOR. We then used the cross-correlation task NOAO.RV.FXCOR to determine the relative velocities between each standard-star spectrum and an arbitrarily chosen reference spectrum (HD 176047 No. 3). The relative

TABLE 3

DEPENDENCE BETWEEN WAVELENGTH ZERO-POINT SHIFTS AND TELESCOPE POSITION

Object	λ_{obs}	$5577.34 - \lambda_{obs}$	Alt.	Azim.
HD $176047_{sky\ No.\ 1}$.....	5577.58	−0.24	79.6	342.0
HD $176047_{sky\ No.\ 2}$.....	5577.45	−0.11	80.2	358.8
HD $196983_{sky\ No.\ 1}$.....	5577.70	−0.36	71.3	304.0
HD $196983_{sky\ No.\ 2}$.....	5577.45	−0.11	80.2	342.1
HD 203638_{sky}	5577.15	+0.19	73.2	99.4
Phoenix set 1.....	5577.66	−0.32	67.4	334.4
Phoenix set 2.1.....	5577.05	+0.29	68.8	18.8
Phoenix set 2.2.....	5577.08	+0.26	64.3	34.6

NOTE.—Values for the Phoenix sets are averages over all the slitlets.

velocities V_{rel} were transformed to $\delta(\log \lambda)$ increments as

$$\delta(\log \lambda) = -V_{rel} \log e/c$$

and added to the CRVAL1 header parameter, which, in a logarithmic wavelength scale, provides the logarithm of the starting spectrum wavelength. Then, we combined the individual spectra into a single, high-S/N template using NOAO.ONEDSPEC.SCOMBINE. By construction, the "heliocentric velocity" of this master template is that of HD 176047, i.e., -42.8 km s^{-1}.

We then used the master template to obtain the *observed* radial velocity of the velocity standards. From the differences between the observed and *true* heliocentric velocity, we can (1) calculate an offset between the radial velocity template and the overall velocity system defined by the standards, which will be applied to the Phoenix velocity measurements to transform them to a *true* heliocentric system, and (2) estimate the mean error with which we are determining the velocities of the standard stars. Because of the higher S/N of the standard-star spectra, this will be a lower limit of the error in the Phoenix velocity determinations. Only the standards for which we had a companion long-exposure sky spectra to correct the zero point of the wavelength calibration have been used for this purpose. Table 2 lists the results of this comparison. The σ_v values have been calculated as described in § 3.3. The σ-weighted mean difference between the true and observed heliocentric velocity is $V_{helio} - V_{obs} = 1.2$ with dispersion $\sigma_V = 1.7$ km s^{-1}.

3.3. *Velocity of Phoenix Giants*

The radial velocities of the Phoenix giants were determined by cross-correlating each star with the master template described in § 3.2 using the IRAF task NOAO.RV.FXCOR. Figure 5 shows the template spectra, an example of a typical Phoenix spectrum, and the corresponding cross-correlation function.

The σ_v errors were determined in the same way as described in Vogt et al. (1995), using six repeated measurements of two standard *plus* two repeated measurements of six Phoenix stars, listed in Table 4. We assumed that the velocity errors can be written as $\sigma_v = \alpha/(1 + R)$, where α is a constant (Tonry & Davis 1979). We then defined the χ^2 statistic for the repeat measurements as $\sum (1 + R_i)^2 (v_i - \langle v \rangle)^2/\alpha^2$ where $\langle v \rangle$ refers to the mean velocity of the star corresponding to observation *i*. We then calculate the α-value that gives a value of χ^2 corresponding to a 50% probability that we would exceed that value of χ^2 by chance (we will denote this value as χ^2_{50}). With this definition, the adopted errors are equivalent to 1 σ Gaussian errors. For this set of 18 observations of eight stars with 10 degrees of freedom, we have $\chi^2_{50} = 0.934$, from which $\alpha = 455$.

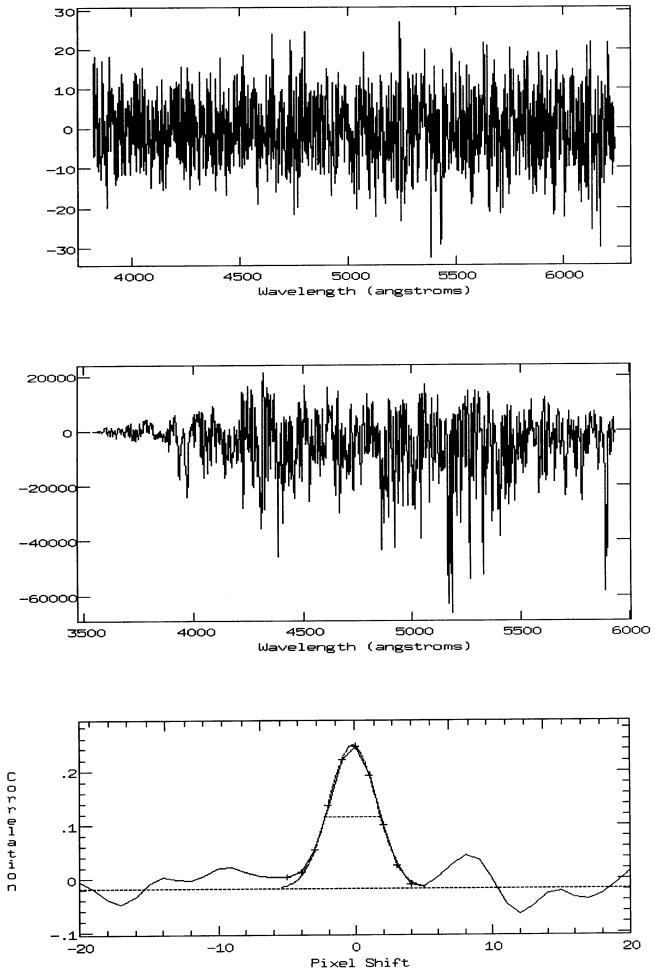


FIG. 5.—*Top*: Extracted spectrum of a typical Phoenix giant (Phoenix set 1–14 in Table 5); *middle*: spectrum of the master radial velocity template; *bottom*: the cross-correlation peak obtained from the top spectrum using the master template. The Tonry-Davis *R*-value for this star is 11.6, which is the median value of all the stars considered in the Phoenix radial velocity derivation.

TABLE 4

SUMMARY OF REPEAT VELOCITY MEASUREMENTS

Star	V_{helio}	R	$\langle V \rangle$	$V_{helio} - \langle v \rangle$
HD 176047 No. 1	−40.8	91.4	−43.2	2.4
HD 176047 No. 2	−46.1	112.6	−43.2	−2.9
HD 176047 No. 3	−42.6	115.8	−43.2	0.5
HD 196983 No. 1	5.2	62.4	−6.7	11.9
HD 196983 No. 2	−15.2	98.4	−6.7	−8.5
HD 196983 No. 3	−10.2	79.6	−6.7	−3.4
Phoenix set 2.1-5	−54.6	8.8	−66.3	11.61
Phoenix set 2.2-5	−77.9	13.4	−66.3	−11.61
Phoenix set 2.1-8	−26.3	10.4	−47.3	21.01
Phoenix set 2.2-8	−68.3	15.4	−47.3	−21.01
Phoenix set 2.1-9	−51.5	8.1	−52.3	0.80
Phoenix set 2.2-9	−53.1	21.1	−52.3	−0.80
Phoenix set 2.1-12.....	−68.0	9.1	−53.9	−14.1
Phoenix set 2.2-12.....	−39.9	13.9	−53.9	14.1
Phoenix set 2.1-14.....	−9.3	9.0	−28.3	19.0
Phoenix set 2.2-14.....	−47.3	18.2	−28.3	−19.0
Phoenix set 2.1-15.....	−30.0	9.8	−44.8	14.8
Phoenix set 2.2-15.....	−59.6	14.5	−44.8	−14.8

Table 5 lists the measured individual heliocentric velocities for the observed Phoenix stars with the corresponding *R*- and σ_v-values. Only stars with well-defined cross-correlation peaks have listed velocities. Some stars in Phoenix set 2 have repeated measurements. Two of the observed stars turned out not to be RGB stars. Their spectra are briefly discussed in the Appendix.

Figure 6 shows that there is no noticeable trend in the measured velocities as a function of V magnitude, $V-I$, color index, position angle P.A., or galactocentric distance r in Phoenix. The σ_v-weighted average of these velocities is -57 ± 6 km s^{-1}, the same as the median velocity. The

TABLE 5

DATA OF THE SPECTROSCOPICALLY OBSERVED STARS IN PHOENIX[a]

Star	α (J2000.0)	δ (J2000.0)	V	$v_{\mathrm{helio_{obs}}}$	R	σ_v	Comment
Phoenix set 1–5	01 50 53.4	−44 25 34.6	21.03	−64.1	10.1	40.9	
Phoenix set 1–6	01 50 55.4	−44 26 43.7	20.71	−60.1	16.9	25.4	
Phoenix set 1–7	01 50 58.1	−44 26 47.7	21.13	−23.7	9.8	42.2	
Phoenix set 1–8	01 50 59.7	−44 26 18.0	21.24	−64.7	17.4	24.7	
Phoenix set 1–9	01 51 02.0	−44 26 15.3	20.94	−84.7	18.9	22.8	
Phoenix set 1–10	01 51 04.1	−44 27 16.6	20.70	−78.3	16.3	26.3	
Phoenix set 1–11	01 51 06.5	−44 26 36.3	20.60	−38.4	27.1	16.2	
Phoenix set 1–12	01 51 08.1	−44 27 03.9	20.76	−57.2	16.7	25.6	
Phoenix set 1–13	01 51 10.7	−44 26 04.8	20.70	−39.0	9.7	42.5	
Phoenix set 1–14	01 51 12.5	−44 27 04.6	21.38	−52.1	11.6	36.1	
Phoenix set 1–15	01 51 14.9	−44 25 41.8	21.02	−68.9	21.3	20.4	
Phoenix set 1–16	01 51 17.1	−44 26 01.2	20.82	−52.0	9.7	42.4	
Phoenix set 1–17	01 51 19.2	−44 26 34.3	20.71	...	...	...	Low S/N
Phoenix set 1–18	01 51 21.2	−44 26 03.1	21.05	...	...	...	Low S/N
Phoenix set 2.2–2	01 51 05.1	−44 29 42.6	21.33	−52.9	8.8	46.2	
Phoenix set 2.2–3	01 51 07.3	−44 29 23.5	21.06	−74.6	8.7	47.0	
Phoenix set 2.2–4	01 51 09.6	−44 29 03.1	20.95	−59.2	7.4	54.0	
Phoenix set 2.1–5	01 51 08.3	−44 28 30.7	20.88	−48.5	8.8	46.2	
Phoenix set 2.2–5				−77.6	13.4	31.5	
Phoenix set 2.2–6	01 51 08.9	−44 28 11.9	20.62	...	...	...	C star
Phoenix set 2.2–7	01 51 10.2	−44 27 48.2	21.21	−19.3	16.6	25.9	
Phoenix set 2.1–8	01 51 06.7	−44 27 22.8	20.73	−26.4	10.5	39.4	
Phoenix set 2.2–8				−66.3	15.6	27.3	
Phoenix set 2.1–9	01 51 08.1	−44 27 03.9	20.72	−50.8	8.2	49.3	
Phoenix set 2.2–9				−51.9	21.4	20.3	
Phoenix set 2.2–10	01 51 02.8	−44 26 45.5	21.03	−92.1	16.1	26.7	
Phoenix set 2.2–10;s2.....	01 51 02.8	−44 26 41.9	21.34	−67.0	14.9	28.6	
Phoenix set 2.2–10;s3.....	01 51 02.7	−44 26 32.3	20.23	...	...	...	Bright supergiant
Phoenix set 2.2–11	01 51 10.8	−44 26 23.9	20.93	−48.3	8.3	48.9	
Phoenix set 2.2–11;s2.....	01 51 10.8	−44 26 20.5	21.72	−88.6	13.8	30.7	
Phoenix set 2.1–12	01 51 05.6	−44 25 52.4	20.85	−68.6	9.1	45.1	
Phoenix set 2.2–12				−39.3	13.8	30.7	
Phoenix set 2.2–13	01 51 08.3	−44 25 34.4	21.27	−51.5	8.8	46.3	
Phoenix set 2.1–14	01 51 04.9	−44 25 10.5	20.78	−15.8	9.2	44.4	
Phoenix set 2.2–14				−46.1	18.6	23.3	
Phoenix set 2.2–15	01 51 04.4	−44 24 42.9	20.72	−58.7	14.4	29.5	
Phoenix set 2.2–16	01 51 10.8	−44 24 24.3	21.33	−44.7	7.9	51.3	
Phoenix set 2.1–18	01 51 12.9	−44 23 41.4	20.61	−41.1	7.7	52.2	
Phoenix set 2.2–18				−50.8	9.9	41.7	

[a] With radial velocities for the RGB stars with sufficient S/N to obtain a well-defined cross-correlation peak.

mean value of the Phoenix velocity remains stable within the errors if we eliminate from the average calculation stars with velocities 3 σ above and below the mean. With this selection, we obtain $V_{\mathrm{Phoenix\text{-}obs}} = -53 \pm 6$ km s^{-1}. After correcting for the difference between the true and measured heliocentric velocity of the standard stars, we conclude that the *true* radial velocity of the stellar component in Phoenix is $V_{\odot} = -52 \pm 6$ km s^{-1}, which we will adopt in the remainder of this paper.

4. DISCUSSION

4.1. *The Stellar Radial Velocity of Phoenix and Its Association with the* H I *Clouds.*

In their paper about the H I in the field of Phoenix, St-Germain at al. (1999; see their Fig. 4) discuss the identification of four components at heliocentric velocities −23, 7, 59, and 140 km s^{-1}. The components at 7 and 140 km s^{-1} are most likely of Galactic and Magellanic Stream origin, respectively. The nature of the other two components is unclear, but St-Germain et al. conclude that the component at −23 km s^{-1} is most likely associated with Phoenix because of (1) its compact structure and partial overlap with the Phoenix stellar component, (2) the amount of H I mass inferred for the cloud at the Phoenix distance, which is similar to the mass of other dSph or dSph/dIrr galaxies, (3) its velocity structure, unlike that of high-velocity clouds, which could indicate either rotation or ejection from Phoenix, and (4) the location of the cloud west of Phoenix, consistent with the propagation from east to west of the most recent star formation event in the galaxy, as discussed in Martínez-Delgado et al. (1999). Our determination of the stellar radial velocity of Phoenix $V_{\odot} = -52 \pm 6$ km s^{-1} tends to support this particular association, if any, between H I in the field of Phoenix and the dwarf galaxy itself. The relatively large velocity difference of gas and stars, however, means that the association is not unquestionable and merits some discussion, as does the particular morphology and location of the H I cloud.

In this section, we will present the results of a series of semianalytical and numerical simulations, under the assumption that the H I cloud at −23 km s^{-1} was once part

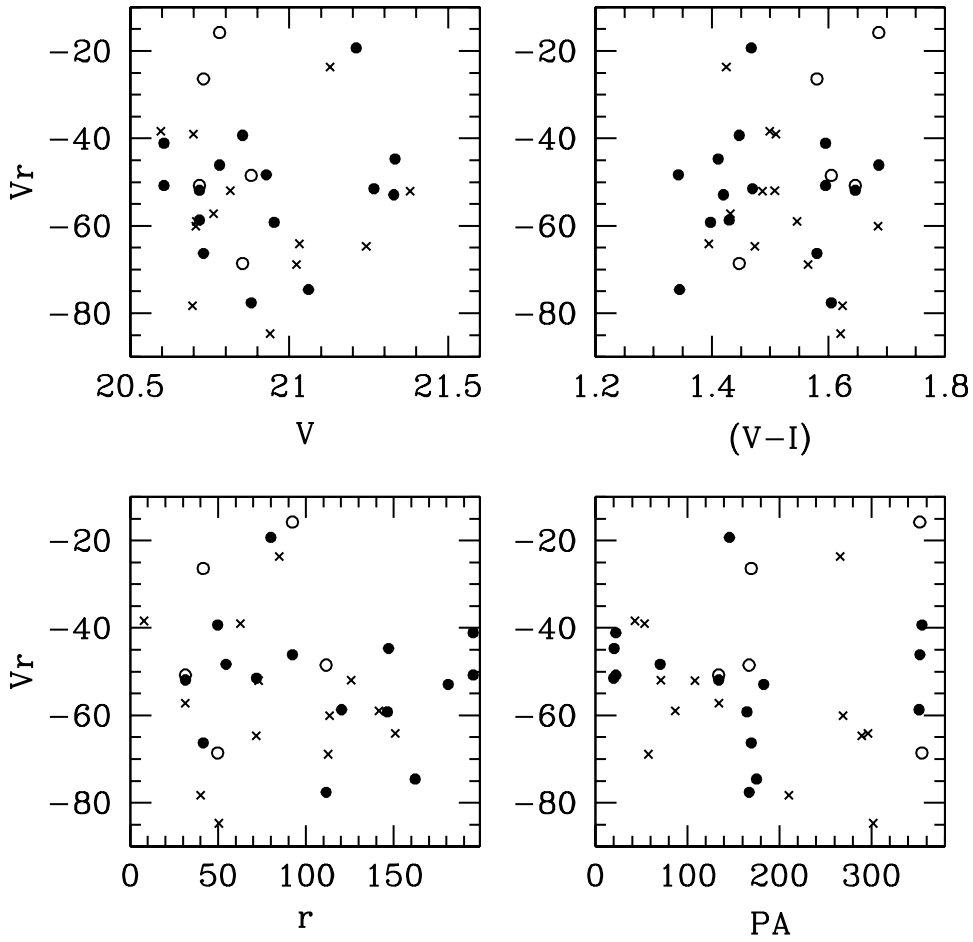


FIG. 6.—Radial velocities of Phoenix stars as a function of a number of parameters. *Clockwise from top left*: V_r vs. V magnitude, V_r vs. $V-I$ color index, V_r vs. position angle (in degrees), and V_r vs. galactocentric distance (in arcseconds) within Phoenix. Crosses correspond to Phoenix set 1, open circles to Phoenix set 2.1, and solid circles to Phoenix set 2.2. Note that no trends in V_r with respect any of these parameters, or with the Phoenix set, exist.

of Phoenix and participated in the last star formation event observed in the galaxy about 100 Myr ago, which is the age of the younger HeB stars found in the western region of Phoenix. We will consider two possible mechanisms that may have stripped Phoenix of its gas: gas ejection by explosions of supernovae (SNe) and by ram pressure stripping. These models allow us to set limits to the necessary conditions for this stripping to have taken place under a given mechanism, and we find that both mechanisms may indeed have been responsible of the observed situation. Similar calculations under the assumption that the H I cloud at $+59$ km s^{-1} was once associated to Phoenix lead to unlikely boundary conditions (very large number of SNe required or large density of the intergalactic medium), which makes us conclude that this one is a chance superposition.

4.1.1. *Gas Ejected by Supernova Explosions*

The possibility that an event of star formation in a small galaxy can actually blow out all or part of its gas has been profusely discussed in the literature from the theoretical point of view (e.g., Mathews & Baker 1971; Larson 1974; Dekel & Silk 1986; Mac Low & Ferrara 1999). This gas removal could eventually halt subsequent star formation and explain the low metallicity observed in dwarf galaxies and the relationship between their total mass and metallicity. Also, the H I mappings of some dwarf galaxies (Puche & Westpfahl 1994) have shown that, in the smallest dwarf irregular galaxies, one large, slowly expanding shell usually dominates the interstellar medium.

In the case of Phoenix, we estimated the energy that should have been injected to the interstellar medium by SN explosions if these were responsible for the ejection of the gas. We assumed that the H I cloud was ejected 100 Myr ago and projected in the opposite direction with respect to the observer (as indicated by the respective observed velocities -52 km s^{-1} and -23 km s^{-1} of Phoenix and H I cloud) and along the trajectory of Phoenix, in such a way that both observed velocities are affected by the same projection angle. We solved the equations of motion, considering only the effect of Phoenix's gravity force and imposing the projected distance between Phoenix and the H I cloud ($d \sim 0.65$ kpc) and their observed radial velocities (-52 and -23 km s^{-1}, respectively) as boundary conditions. This calculation allows us to simultaneously estimate the energy necessary to eject the gas, $E_{\rm SNe} \sim 2 \times 10^{51}$ ergs and the most likely angle between the line of sight and the line connecting Phoenix and the H I cloud, $\alpha \sim 10°$.

To estimate the number of SNe necessary to inject this energy into the interstellar medium, we should estimate what fraction of the energy of a supernova is actually transferred as kinetic energy to the gas. Larson (1974) showed that the thermal energy available per SN for driving a galactic wind in cases where SN remnant cooling is impor-

tant (as would be the case for dwarf galaxies) is of the order of 10^{50} ergs, i.e., about 10% the total energy output of the SNe. In the case of Phoenix, therefore, about 20 SNe would have been necessary to produce the inferred energy. By comparing the number of observed 100 Myr old stars in the main sequence of Phoenix with the number predicted by synthetic CMDs, Martínez-Delgado et al. (1999) calculate that the total mass involved in the burst of star formation that produced the younger stellar association in the western part of the galaxy is $1.8 \times 10^4\ M_\odot$. Using the initial mass function of Kroupa, Tout, & Gilmore (1993), we derive that ~ 50 stars more massive that 10 $M_\odot$ should have been produced during that event, providing a potential number of SNe large enough to produce the necessary energy to have blown away the gas.

The most likely estimated angle, $\alpha \sim 10°$, between the line of sight and the line connecting Phoenix and the H I cloud means that both objects are in almost radial trajectories with respect to the line of sight. Therefore, their total velocities are very similar to the projected component, and the actual distance between Phoenix and the H I cloud is about 3.5 kpc. Considering this distance and the relative velocities of the H I cloud and Phoenix, a Phoenix total mass $M_{\text{Phoenix-tot}} \sim 4 \times 10^8\ M_\odot$ would be necessary if the H I cloud were to be gravitationally bound to Phoenix. This is about 1 order of magnitude larger than the total mass estimated for Phoenix, $\sim 3.3 \times 10^7\ M_\odot$ (Mateo 1998), which would imply that $(M/L)_{\text{Phoenix}} \sim 400\ (M/L)_\odot$ and indicates that indeed the amount of energy produced by the last burst of star formation would have been large enough to blow away the small amount of gas remaining in the galaxy after that particular episode of star formation.

This model of SN-driven winds, even though very convincing from the energetic point if view, has the drawback of the regular appearance of the H I cloud and the highly anisotropic geometry of the gas-stars configuration, with all the gas out in one direction in a single isolated cloud. These are not a problem for the ram pressure hypothesis discussed in the next section.

4.1.2. *Ram Pressure Stripping*

The gas of the intergalactic medium (IGM) produces a ram pressure on the gas of an object (satellite) moving through it, such that

$$P_{\text{ram}} \propto \rho_{\text{IGM}} v^2\ , \qquad (1)$$

where ρ_{IGM} is the gas density of the IGM and v is the velocity of the satellite (Gunn & Gott 1972) relative to the IGM. When the pressure is strong enough, the gas of the satellite is slowed down and stripped from the satellite. We have simulated a gas-rich dwarf galaxy moving through a gaseous environment, using a semianalytical approach to model the ram pressure stripping (see Gómez-Flechoso 2001 for details of the numerical models). We have analyzed the conditions for the H I cloud to be stripped by the IGM. We assumed an ambient medium of uniform density and at rest with respect to the Galaxy, a peak of the gas density of the H I cloud of 4×10^{19} atoms cm^{-2} and the total luminosity of Phoenix of $L_B = 9.5 \times 10^5\ L_\odot$ (St. Germain et al. 1999). Different mass-to-light ratios have been considered for the dwarf galaxy in our simulations. As in the previous section, we reproduce the observational velocities and positions of Phoenix and the H I cloud, assuming that (1) the gas has been stripped along the trajectory and (2) the ram pressure started 100 Myr ago. In this case, the forces involved in the trajectory of the cloud are the gravitational force of the dwarf galaxy and the ram pressure stripping force due to the IGM. The latter is produced by the ram pressure given by equation (1), taking into account that the velocity v in the equation is the velocity relative to the IGM, which is the Galactocentric velocity. The Galactocentric radial components of the velocity of Phoenix and the H I cloud are $V^{\text{GC}}_{R,\text{Phe}} = -144$ km s^{-1}, and $V^{\text{GC}}_{R,\text{H I}} = -115$ km s^{-1}, respectively. As in the calculation relative to the SNe in the previous section, in order to reproduce the projected distance between Phoenix and the H I cloud and their Galactocentric radial velocities, we estimate the angle, α, between the line of sight and the trajectory of the satellite, and the gas density of the environment, ρ_{IGM} (assuming it is nearly constant). The best model corresponds to $\alpha \sim 21°$, roughly independent of the mass-to-light ratio of Phoenix, and $\rho_{\text{IGM}} \sim (2.0\text{–}3.0) \times 10^{-4}$ atoms cm^{-3}, for $(M/L)_{\text{Phoenix}} = 2\text{–}20\ (M/L)_\odot$. This value of α implies that (1) the orbit of Phoenix is quite eccentric, (2) the true distance between Phoenix and the H I cloud is about 1.8 kpc, and (3) the total velocity of Phoenix and the H I cloud are $V^{\text{GC}}_{\text{Phe}} \simeq -154$ km s^{-1} and $V^{\text{GC}}_{\text{H I}} \simeq -123$ km s^{-1}. The value of the gas density of the environment, $\rho_{\text{IGM}} = (2.0\text{–}3.0) \times 10^{-4}$ atoms cm^{-3}, obtained in this case is consistent with some estimates of the hot gas density of a Local Group halo (Suto et al. 1996; but see also Murali 2000; Mulchaey 2000 and references therein).

In Figure 7, we show the results of the simulation: the gray levels refer to the predicted velocity of the gas (darker corresponds to more negative values of the velocity) and the white contours correspond to heliocentric radial velocities -27, -24, -21, and -18 km s^{-1}. The black contours correspond to the predicted gas density (3.5, 3.0, 2.5, 2.0, and 1.5×10^{19} cm^{-2}). The structure of the gas in the simulations remains quite smooth as it is stripped from the satellite, keeping a distribution similar to the observed H I cloud. Note also that (1) a velocity gradient in the sense that the most extreme differences in velocity are seen farthest from the galaxy and (2) the velocity of the stripped gas is closer to the systemic velocity of the Milky Way than that of Phoenix are predicted by our model (see also Blitz & Robishaw 2000), in agreement with the observed Phoenix parameters.

These arguments support the hypothesis of the ram pressure as responsible of the gas stripping in Phoenix. However, it may demand Phoenix to be in its first approach to the Galactic center, which may be possible if Phoenix is not bound to the Milky Way or is in a very long period orbit. Given its almost radial orbit, near the pericenter Phoenix must cross zones with a much larger gas density than in its current position, and at much larger velocity with respect to the IGM. This would imply a much larger ram pressure stripping, to which the gaseous content of the galaxy could have only survived if it originally was very massive and concentrated, unlike at the present time.

There are at least a couple of theoretical works that consider tidal stripping of a gaseous satellite approaching to the Milky Way. They suggest that such a survival in the close approach may not be completely unrealistic. Mayer et al. (1999, 2001) show that low surface brightness satellites of a Milky Way–like galaxy, in eccentric orbits (as typical in hierarchical models of galaxy formation), may lose up to 90% of their stellar mass due to tidal stripping. But, could any amount of gas remain still bound to the galaxy after

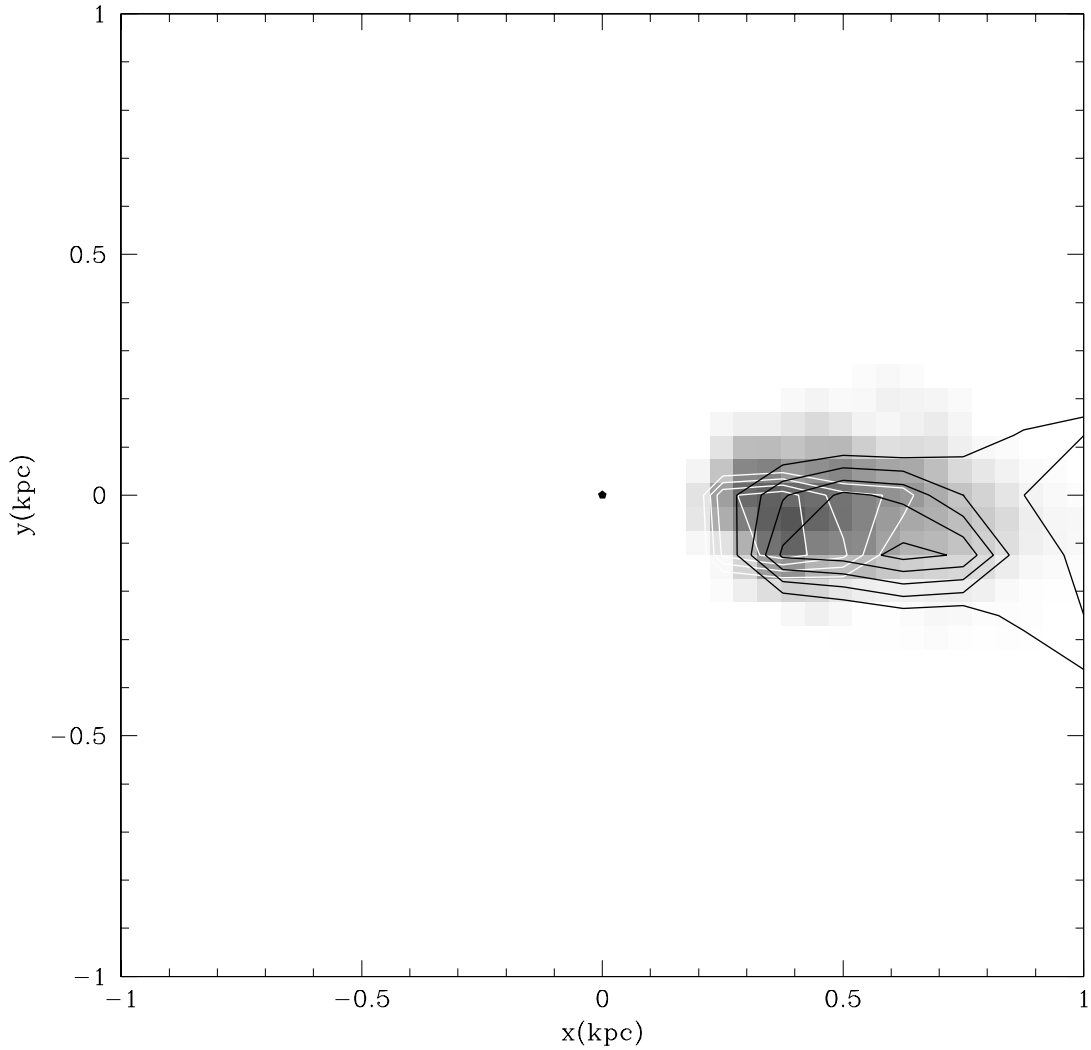


FIG. 7.—Results of the ram pressure stripping simulation: gray levels refer to the predicted H I velocity (darker corresponds to more negative values of the velocity), and white contours correspond to heliocentric radial velocities −27, −24, −21, and −18 km s^{-1}. The black contours show the predicted gas density (3.5, 3.0, 2.5, 2.0, and 1.5 × 10^{19} cm^{-2}).

one or more pericentric passages? Lin & Murray (1998) argue that "around the dSph galaxies in the Galactic halo, their ejected unbound gas follows their orbits analogous to the Magellanic Stream. Gas density declines/enhances near peri/apogalacticon as the stream is stretched/compressed (by tidal forces). At apogalacticon, where the density is at a maximum and exposure to the Galactic UV flux is at a minimum, the diffuse gas can recombine to form atomic and molecular hydrogen and eventually stars." To assess the plausibility of these different alternatives when ram pressure is included in the case of Phoenix, it would be necessary to perform much more detailed simulations, which exceed the scope of the present paper. In any case, gas loss will be maximum at the pericenter, where both tidal stripping and ram pressure forces are larger.

4.2. *Comparison with Observations of Other Dwarf Galaxies*

In two cases, DDO 210 and LGS 3, for which H I superposed on the stellar component had been observed, Blitz & Robishaw (2000) detect a stronger emission component offset from the stellar component. They also find H I possibly associated with Leo I, whose position is also offset from the stellar component. Leo I and LGS 3, for which an optical velocity is also known, present interesting similarities with the Phoenix case. In LGS 3, H I cloud and galaxy differ in velocity by about 50 km s^{-1}, which implies that they are not gravitationally bound. In the case of Leo I, the velocity centroid of the emission that seems more closely associated with the galaxy (both spatially and kinematically) differs by about 30 km s^{-1} from the velocity of the stellar component. Apart from the magnitude of the difference in velocity between gas and stars, Leo I, LGS 3, and Phoenix are similar also in (1) the morphology of the gas relative to the stars and (2) the time of the last events of star formation, which is of the order of a few hundred million years in all of them (Phoenix, Martínez-Delgado et al. 1999; Leo I, Gallart et al. 1999a, 1999b; LGS 3, Aparicio, Gallart, & Bertelli 1997b). For Leo I and LGS 3, Blitz & Robishaw (2000) discuss the possibility that the H I has been stripped by the ram pressure of the hot (Galactic or M31) halo gas. Despite a distance to the Milky Way of almost twice that of Leo I, this seems a plausible explanation also for Phoenix, as we have discussed in § 4.1.2.

4.3. *Phoenix as a Milky Way Satellite and the Mass of the Galaxy*

The minimum required mass of the Milky Way for Phoenix to be bound (based on the values of the Galacto-

centric velocity of Phoenix and its distance to the Galactic center obtained above) is $M_{MW}(<450 \text{ kpc}) \geq 1.2 \times 10^{12} M_{\odot}$. This value comfortably fits within most current estimates of the Milky Way mass (see Zaritsky 1999 for a review). For example, Zaritsky et al. (1989) conclude that $M_{MW} = (1.3 \pm 0.2) \times 10^{12} M_{\odot}$ from timing arguments involving Leo I and the Milky Way; on the other hand, Anguita, Loyola, & Pedreros (2000) calculate, from a recent LMC proper-motion measurement that $M_{MW} = (3\text{–}4) \times 10^{12} M_{\odot}$ out to 50 kpc, if the LMC is to be bound to the Milky Way (see also Méndez et al. 1999). We conclude therefore that Phoenix is very likely the outermost (known so far) Milky Way satellite.

5. SUMMARY AND CONCLUSIONS

We have presented the first measurement of the radial velocity of the Phoenix stellar component, using FORS1 in MOS mode at the VLT UT1 (Antu) telescope. We have obtained spectra of 31 RGB stars. Two additional stars for which we obtained spectra turned out to be a carbon star and a bright supergiant star (see Appendix). From the spectra of the RGB stars we derive a heliocentric optical radial velocity of Phoenix $V_{\odot} = -52 \pm 6$ km s^{-1}. On the basis of this velocity and taking into account the results of a series of semianalytical and numerical simulations, we discuss the possible association of two of the four H I clouds observed in the Phoenix vicinity, those at velocities -23 and $+59$ km s^{-1}, which are not associated with either the Milky Way or the Magellanic Stream (St-Germain et al. 1999; Young & Lo 1997; Oosterloo et al. 1996).

We conclude that the characteristics (mass, distance, velocity relative to Phoenix) of the H I cloud with heliocentric velocity -23 km s^{-1} are consistent with this gas having been associated with Phoenix in the past, until the last event of star formation in the galaxy, about 100 Myr ago. Two possible scenarios for the loss of this gas are discussed: its ejection by the energy released by the SNe produced in that last event of star formation, and a ram pressure stripping scenario. The assumption that the H I cloud at $+59$ km s^{-1} was once associated to Phoenix leads to unlikely boundary conditions (very large number of SNe required or large density of the IGM), which makes us conclude that this one is a chance superposition.

We derive that the kinetic energy necessary to eject the gas is $E_{SNe} \sim 2 \times 10^{51}$ ergs. The number of SNe necessary to transfer the inferred amount of kinetic energy to the gas cloud is consistent with the total mass involved in the last event of star formation $\sim$100 Myr ago by Martínez-Delgado et al. (1999). Considering the derived distance between Phoenix and the H I cloud and their relative velocities, the Phoenix total mass necessary for the H I cloud to be gravitationally bound is about an order of magnitude larger than the total mass estimated for Phoenix. This indicates that the amount of energy produced by the last burst of star formation would have been large enough to blow away the small amount of gas remaining in the galaxy after that particular episode of star formation. The main drawbacks of this SN-driven winds scenario are the regular appearance of the H I cloud and its anisotropic distribution with respect to the stellar component. Another possibility is that the H I gas observed at -23 km s^{-1} was stripped as a consequence of ram pressure by the IGM. In our simulations, the structure of the gas remains quite smooth as it is stripped from Phoenix, keeping a distribution similar to that of the observed H I cloud.

Since both the SNe and ram pressure stripping scenarios for gas ejection in Phoenix are consistent with the observations, a combined scenario may be also plausible. One possibility is that supernovae resulting from a burst of star formation diluted the gas in Phoenix and increased its energy enough for it to be swept away by an already existing intergalactic wind. Another possibility is that Phoenix may be crossing regions of variable gas density, and that 500–100 Myr ago it ran into a relatively dense clump or stream of intergalactic gas that was responsible for the sweeping event that presumably terminated—or temporarily halted—the star formation.

Finally, we discuss the possibility that Phoenix may be a bound Milky Way satellite. The minimum required mass of the Milky Way for Phoenix to be bound is $M_{MW}(<450 \text{ kpc}) \geq 1.2 \times 10^{12} M_{\odot}$. This value comfortably fits within most current estimates of the Milky Way mass.

It is a pleasure to thank I. Perez, R. Guzman, E. Hardy, and S. Zepf for very useful discussions on spectroscopic reductions and to R. Larson and L. Mayer for enjoyable conversations about possible scenarios for gas stripping and for a critical reading of the manuscript. J. Mulchaey and S. G. Navarro pointed us to useful references on gas in

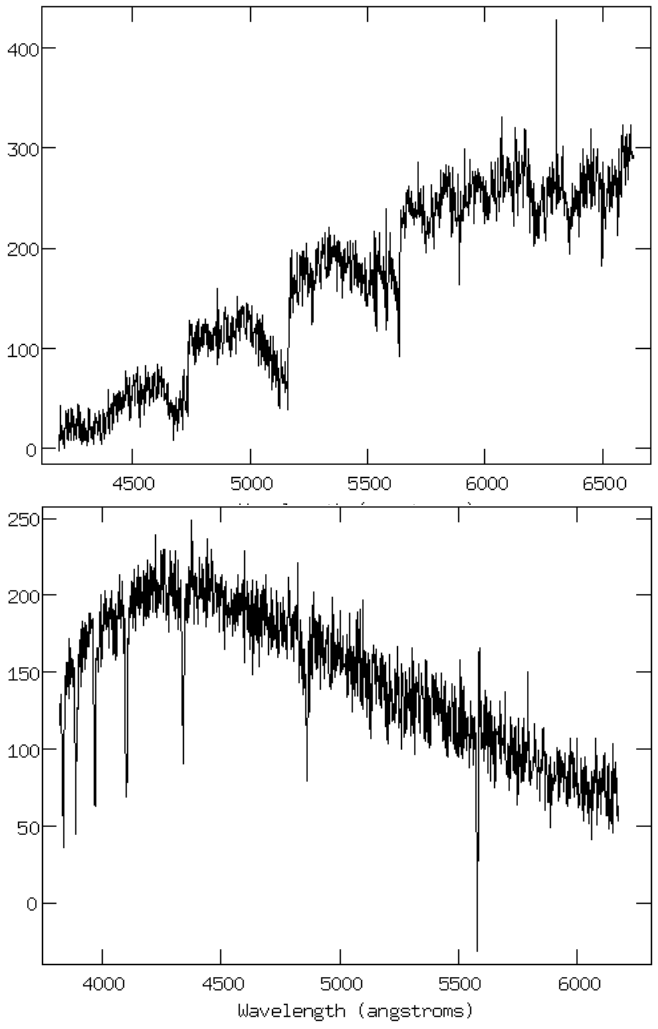


FIG. 8.—*Top*: Spectrum of a carbon star in Phoenix (Phoenix set 2.2–6 in Table 5); *bottom*: spectrum of a young star in Phoenix (Phoenix set 2.2–10s3), probably a bright giant (luminosity class II) of early-A spectral type.

galaxy groups and spectral classification, respectively. We also thank A. Iovino, for taking an image of Phoenix the night before our observations which allowed us to produce an accurate MOS setup. T. Szeifert and H. Boehnhardt provided advice at the telescope which ensured the success of the observations. Support for this work was provided by Chilean CONICYT grant 1990638, NASA grant GO-5350-03-93A and by the IAC through grant PB3-94.

APPENDIX

A YOUNG STAR AND A CARBON STAR SPECTROSCOPICALLY CONFIRMED (SERENDIPITOUSLY) IN PHOENIX

One of the stars originally selected as a candidate RGB star, Phoenix set 2.2–6, as well as Phoenix set 2.2–10;s3 (Table 5) turned out to be other types of stars.

Phoenix set 2-6 (Fig. 8*a*) has the spectra typical of a carbon star (see, e.g., Cannon, Niss & Nørgaard-Nielsen 1981 for sample spectra and discussion of the features present in a C star spectrum). It is one of the two C stars previously confirmed spectroscopically by Da Costa (1994). It is the brightest red star in our sample, located above the TRGB (identified in the CMD in Fig. 4, *filled square*).

Phoenix set 2.2-10;s3 (Fig. 8*b*) was not in our original candidate list. It was included in the extreme of one of the slitlets, and turned out to be a young star. Its spectra clearly shows the series of Balmer lines in absorption, and at this low resolution, low S/N, we can classify it in the range of spectral types B5–A5 (Jacoby, Hunter, & Christian 1984). Using $(m - M)_0 = 23.0$ and $A_V = 0.06$ for Phoenix (Martínez-Delgado et al. 1999), the absolute magnitude for this star, *if* it belongs to Phoenix, is $M_V = -2.83$ (Table 5), which would correspond to a bright giant star of luminosity class II, and probably early A spectral type (Schmidt-Kaler 1982). The position of this star in the CMD is consistent with a blue loop star with $Z = 0.001$ and age 100 Myr, formed in the last event of star formation in Phoenix.

REFERENCES

Anguita, C., Loyola, P., & Pedreros, M. H. 2000, AJ, 120, 845
Aparicio, A., Gallart, C., & Bertelli, G. 1997a, AJ, 114, 669
———. 1997b, AJ, 114, 680
Binggeli, B. 1994, in Panchromatic View of Galaxies, ed. G. Hensler, C. Theis, & J. Gallagher (Gif-sur-Yvette: Ed. Frontières), 173
Blitz, L., & Robishaw, T. 2000, ApJ, 541, 675
Cannon, R. D., Niss, B., & Nørgaard-Nielsen, H. U. 1981, MNRAS, 196, 1P
Carignan, C., Beaulieu, S., Côté, S., Demers, S., & Mateo, M. 1998, AJ, 116, 1690
Carignan, C., Demers, S., & Côté, S. 1991, ApJ, 381, L13
Da Costa, G. S. 1994, in ESO/OHP Workshop on Dwarf Galaxies, ed. G. Meylan & P. Prugniel (Garching: ESO), 221
Davies, J. I., & Phillips, S. 1989, Ap&SS, 157, 291
Dekel, A., & Silk, J. 1986, ApJ, 303, 39
Einasto, J., Saar, E., Kaasik, A., & Chernin, A. D. 1974, Nature, 252, 111
Ferrara, A., & Tolstoy, E. 2000, MNRAS, 313, 291
Foster, K. W., et al. 1999, The Astronomical Almanac (Washington: US Nav. Obs.)
Gallart, C., Freedman, W. L., Aparicio, A., Bertelli, G., & Chiosi, C. 1999a, AJ, 118, 2245
Gallart, C., et al. 1999b, ApJ, 514, 665
Gómez-Flechoso, M. A. 2001, in preparation
Gunn, J. E., & Gott, J. R., III. 1972, ApJ, 176, 1
Held, E. V., Saviane, I., & Momany, Y. 1999, A&A, 345, 747
Jacoby, G. H., Hunter, D. A., & Christian, C. A. 1984, ApJS, 56, 257
Kroupa, P., Tout, C. A., & Gilmore, G. 1993, MNRAS, 262, 545
Lacey, C., & Silk, J. 1991, ApJ, 381, 14
Larson, R. B. 1974, MNRAS, 169, 229
Lin, D. N. C., & Faber, S. M. 1983, ApJ, 266, L21
Lin, D. N. C., & Murray, S. D. 1998, in Dwarf Galaxies and Cosmology, ed. T. X. Thuân, C. Balkowski, V. Cayatte, & J. Trân Thanh Vân (Gif-sur-Yvette: Ed. Frontières), 433
Lo, K. Y., Sargent, W. L. W., & Young, K. 1993, AJ, 106, 507
Mac Low, M.-M., & Ferrara, A. 1999, ApJ, 513, 142
Martínez-Delgado, D., Gallart, C., & Aparicio, A. 1999, AJ, 118, 862
Mateo, M. 1998, ARA&A, 36, 435
Mathews, W. G., & Baker, J. C. 1971, ApJ, 170, 241
Maurice, E., et al. 1984, A&AS, 57, 275
Mayer, L., Governato, F., Colpi, M., Moore, B., Quinn, T. R., & Baugh, C. M. 1999, in ASP Conf. Ser. 187, The Evolution of Galaxies on Cosmological Timescales, ed. J. E. Beckman & T. J. Mahoney (San Francisco: ASP)
Mayer, L., Governato, F., Colpi, M., Moore, B., Quinn, T., Wadsley, J., Stadel, J., & Lake, G. 2001, ApJ, 547, L123
Méndez, R. A., Platais, I., Girard, T. M., Kozhurina-Platais, V., & van Altena, W. F. 1999, ApJ, 524, L39
Mulchaey, J. S. 2000, ARA&A, 38, 289
Murali, C. 2000, ApJ, 529, L81
Oosterloo, T., Da Costa, G. S., & Staveley-Smith, L. 1996, AJ, 112, 1969
Osterbrock, D. E., Fulbright, J. P., Martel, A. R., Keane, M. J., Trager, S. C., & Basri, G. 1996, PASP, 108, 277
Puche, D., & Westpfahl, D. 1994, in ESO/OHP Workshop on Dwarf Galaxies, ed. G. Meylan & P. Prugniel (Garching: ESO), 273
Schmidt-Kaler, T. 1982, in Landolt-Börnstein New Series, Group 6, Vol. 2b, Stars and Star Clusters, ed. K. Schaifers & H. H. Voigt (Berlin: Springer), 1
Silk, J. Wyse, R. F. G., & Shields, G. A. 1987, ApJ, 322, L59
Stetson, P. B., Hesser, J. E., & Smecker-Hane, T. A. 1998, PASP, 110, 533
St-Germain, J., Carignan, C., Côté, S., & Oosterloo, T. 1999, AJ, 118, 1235
Suto, Y., Makishima, K., Ishisaki, Y., & Ogasaka, Y. 1996, ApJ, 461, L33
Tonry, J., & Davis, M. 1979, AJ, 84, 1511
van den Bergh, S. 1994, ApJ, 428, 617
Vogt, S. S., Mateo, M., Olszewski, E. W., & Keane, M. J. 1995, AJ, 109, 151
Young, L. M., & Lo, K. Y. 1997, ApJ, 490, 710
Young, L. M., & Lo, K. Y. 1997, 490, 710
Zaritsky, D. 1999, in ASP Conf. Ser. 165, The Third Stromlo Symposium, ed. B. K. Gibson, T. S. Axelrod, & M. E. Putman (San Francisco: ASP), 34
Zaritsky, D., Olszewski, E. W., Schommer, R. A., Peterson, R. C., & Aaronson, M. 1989, ApJ, 345, 759